

THE CONTROL OF AN AC TO HF-AC RESONANT LINK CONVERTER

Miro Milanovič, Robert Kovačič, Franc Mihalič, Rudi Babič
University of Maribor,
Faculty of Electrical Engineering and Computer Science, Slovenia

Keywords: voltage converters, HF-AC AC resonant link converters, UPS, uninterruptible power supplies, DC-DC converters, circuit modelling, circuit analysis, injected-absorbed current method, pulse width modulation, analog control, resonant circuits, high efficiencies

Abstract: The term HF-AC Resonant Link Converters usually denotes a circuit, whose main part is a resonant tank circuit. The main goal of designers of such circuits is to reach a constant magnitude of output voltage with constant frequency and independence of load conditions. In this paper the possibility of maintenance of the constant HF-AC voltage on parallel resonant circuits (frequency 25 kHz) from main supply will be considered. In the family of AC to HF-AC Resonant Link Converters the proposed circuit is quite new. This goal has been reached by providing the energy from main supply by using the accordance between the serial and parallel resonance of the chosen circuit.

Analogna regulacija visokofrekvenčnega AC-AC resonančnega pretvornika

Ključne besede: pretvorniki napetostni, HF-AC AC pretvorniki s povezavo resonančno, UPS napajalniki brez prekinitve, DC-DC pretvorniki, modeliranje vezij, analize vezij, metoda toka injiciranega-absorbiranega, modulacija impulzno širinska, regulacija analogna, krogi resonančni, izkoristki visoki

Povzetek: Pretvorniki, ki so danes v široki uporabi, delujejo v stikalnem režimu ter preklapljajo pri polni napetosti in toku, se pogosto uporabljajo v mnogih aplikacijah, npr. UPS (viri za neprekinjeno napajanje), v reguliranih elektromotornih pogonih, DC/DC pretvornikih itd. S ciljem eliminacije nizkofrekvenčnih spektralnih komponent v izhodni napetosti sistema UPS, nizkofrekvenčnih motenj v momentu električnih motorjev in valovitosti v izhodni napetosti DC/DC pretvornikov, potrebujemo visokofrekvenčni napajalni vir. Takšen visokofrekvenčni vir pa ima zaradi dokaj velikih frekvenc delovanja znatne stikalne izgube. Problem rešujemo z vpeljavo resonančnih oz. kvaziresonančnih principov delovanja v obstoječe pretvornike. Pri uporabi omenjenega principa so mnogi avtorji predlagali vezja, ki v svojih strukturah vsebujejo dvosmerna stikala. V predlaganem vezju resonančnega pretvornika bodo za pretvorbo, ki jo izvede mrežni pretvornik, uporabljena enosmerna stikala. Pretvornik bo deloval s frekvenco 25kHz. Energija bo iz mrežnega dela posredovana paralelnemu resonančnemu krogu skozi serijski resonančni pojav. Ob prehodu napetosti in/ali toka skozi ničelno vrednost izklapljammo polprevodniška stikala v teh pretvornikih. Pretvorniki, zgrajeni na tem principu, se imenujejo "resonančni pretvorniki". S resonančnimi pretvorniki lahko dosežemo izkoristek pretvorbe nad 90%.

1. Introduction

Hard switch converter/inverter technique with high frequency switch is often utilised for many applications (UPS, Variable Speed Electrical Motor Drives, DC-DC Power Supply ect.). In order to get low harmonics contains in output voltage for UPS, low harmonics disturbance in torque of Electrical Motor Drive and low ripple in DC-DC supply units the high frequency is required. Unfortunately, on the contrary the converter/inverter switching losses increase enormously with higher frequency. Introducing resonant or quasi-resonant operation principle into known converters/inverters topology represents the possible solution of this problem. A lot of authors reported about the utility of such principles in wide at the area of Power Electronics [1, 2, 3]. The essential idea of our approach to resonant tank circuit problem is to provide the energy through serial resonant circuits into parallel resonant tank circuits in order to maintain the constant value of output voltage.

2. The novel circuit

The basic scheme for "evolution" of the proposed new circuits is shown in Fig. 1. The circuit represents a "half

wave" configuration which is known from the rectifier's theory. Operation of such circuit is not too complicated. In steady state conditions (the parallel resonant circuits L_1 and C_1 operate and provide the energy to the resistor R_L), transistor Q_1 should be switched on when the parallel resonant link voltage crosses zero as shown in Fig. 5 (not necessary condition). Then L_{11} with elements of parallel resonant tank circuits L_1 and C_1 establishes serial resonant tank circuits. The current through transistor Q_1 is supposed to be in sinusoidal wave shape. When the current crosses zero, diode D_1 switches off and transistor Q_1 can be switched off as well. The soft switch operation is evident.

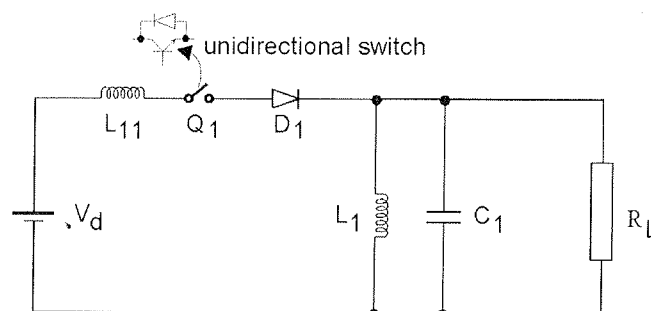


Fig. 1: The "half-wave" resonant link converter configuration

Operation of the circuit from Fig. 2 is quite similar. In that case the conducting losses are lower. In that circuit the energy is providing from DC supply to parallel resonant link in both half periods of AC high frequency voltage.

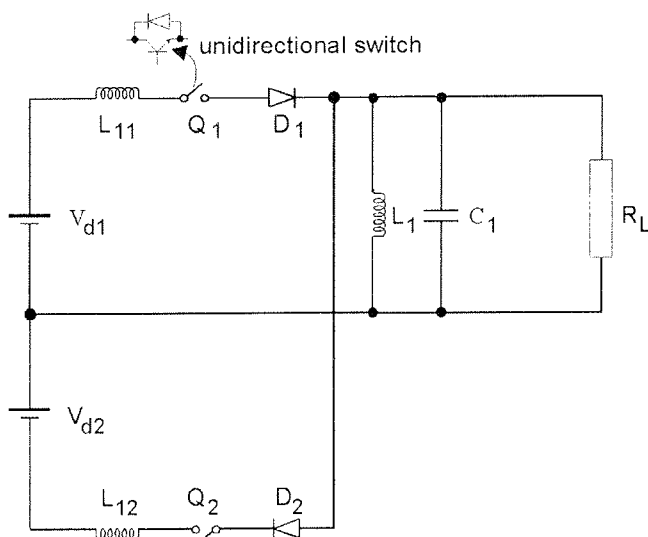


Fig. 2: The "full-wave" resonant link converter configuration

The 3rd circuit (Fig. 3) has been done like the last step of "evolution" of the first circuit (Fig. 1) which we would like to present in this paper. The voltage sources V_{d1} and V_{d2} have been simply replaced by diode bridge and main supply. The new circuit consists of a diode rectifier, two serial inductance (L_{11} and L_{22}), two transistors (Q_1 and Q_2) and two serial diodes which are not necessary for circuit operations because their functions can be taken over by diodes from rectifier bridge.

The converter which in first step operates like DC to HF Resonant Link Converter, in the last step becomes the converter which converts Three Phase Main supply into AC-HF voltage. For tests and operations the voltage of

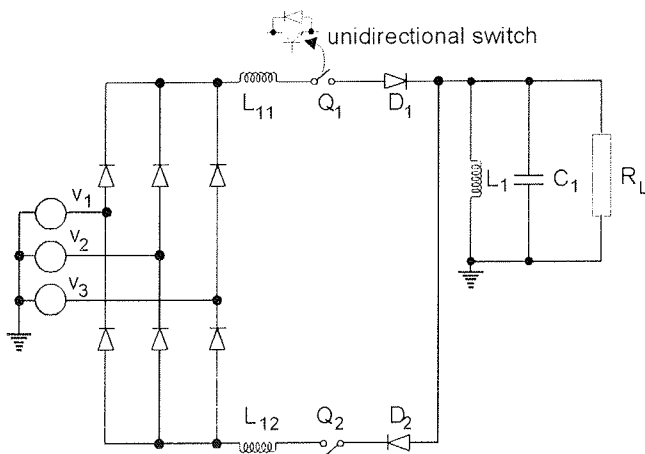


Fig. 3: The AC to HF-AC resonant link converter configuration

HF link, $V_{out} = 1000 V_{p-p}$, frequency, $f_{out} = 22 \text{ kHz}$ and $P_{out} = 500 \text{ W}$ has been chosen.

3. The start-up procedure

The most convenient way to analyse the start-up behaviour is to find out the equivalent circuit from circuit in Fig. 3. It is not difficult to see that the circuit in Fig. 1 represents that circuit. The circuit in Fig. 1 can be called a DC/(half wave) HF-AC resonant converter, because of the similarity in structure with AC/DC diode rectifier. The only difference between these two circuits is in wave shape of supply voltage. In regard to simplify analysis, the response of DC voltage will be discussed. The DC voltage on "+" terminal of diode bridge (Fig. 3) can be computed from the following equation.

$$V_d = \frac{3}{\pi} \hat{V}_1 \quad (1)$$

The original circuit (Fig. 1) will be described by a set of equations (2). These equations describe the behaviour of circuit in Fig. 3 as well. Let us suppose that the voltage V_d is constant and the step response of the circuit can be observed. The current responses are shown in Fig. 4.

The response where zero current crossing has been reached is very interesting because there is any free-wheeling diode needed which should correspond with the energy in inductance L_{11} . If the zero crossing condition trough L_{11} has not been reached there can be a voltage spike on the transistor Q_1 and the circuit can not operate.

$$\begin{aligned} \frac{di_{L11}}{dt} &= \frac{1}{L_{11}} (V_d - v_C) \\ \frac{di_{L1}}{dt} &= \frac{1}{L_1} v_C \\ \frac{di_{L11}}{dt} &= \frac{1}{C} \left(i_{L11} - i_{L1} - \frac{1}{R} v_C \right) \end{aligned} \quad (2)$$

The above system can be solved for two different time intervals. Equations (3), (4) and (5) represent the solution of system of equations (2) in time interval (t_0, t_1), (Fig. 5)

$$i_{L11} = \frac{V_d}{\omega_{os} L_{11}} \left[\frac{L_{11}}{L_{11} + L_1} \omega_{os} t + \frac{L_{11}}{L_{11} + L_1} e^{-\frac{t}{2RC}} \sin(\omega_{os} t + \varphi) \right] - \quad (3)$$

$$I_{co} \frac{L_{11}}{L_{11} + L_1} \left[1 - e^{-\frac{t}{2RC}} \cos(\omega_{os} t + \varphi) \right]$$

$$\begin{aligned} i_{L1} &= \frac{V_d}{\omega_{os} L_{11}} e^{-\frac{t}{2RC}} \sin(\omega_{os} t + \varphi) \\ &+ I_{co} e^{-\frac{t}{2RC}} \cos(\omega_{os} t + \varphi) \end{aligned} \quad (4)$$

$$v_C = V_d \frac{L_{11}}{L_{11} + L_1} \left[1 - e^{-\frac{t}{2RC}} \cos(\omega_{os}t + \varphi) \right] + \frac{I_{co}}{\omega_{os}C} e^{-\frac{t}{2RC}} \sin(\omega_{os}t + \varphi) \quad (5)$$

and equations (6) and (7) represent the solutions of system of equations (2) in time interval (t₁,t₂) (Fig. 5):

$$i_{L1} = I_{C1} e^{-\frac{t}{2RC}} \cos(\omega_{op}t + \varphi) - V_d C \omega_{op} e^{-\frac{t}{2RC}} \sin(\omega_{op}t + \varphi) \quad (6)$$

$$v_C = V_d e^{-\frac{t}{2RC}} \cos(\omega_{op}t + \varphi) + \frac{I_{C1}}{\omega_{op}C} e^{-\frac{t}{2RC}} \sin(\omega_{op}t + \varphi) \quad (7)$$

where:

$$\omega_{os} = \frac{1}{\sqrt{L_N C}}, \quad L_N = \frac{L_{11} L_1}{L_{11} + L_1}, \quad \omega_{op} = \frac{1}{\sqrt{L_1 C}}$$

$$\varphi = \arctg\left(\frac{Z_s}{R}\right), \quad Z_s = \sqrt{\frac{L_N}{C}}$$

If the appropriate value for L₁₁ has been chosen, the current i_{L11} should not exceed the transistor current limit and the parallel resonant tank circuit gets enough energy and oscillation starts with its own parallel resonant frequency.

The current i_{L11} starts to flow when the switch Q₁ is ON. That current has a sinusoidal wave-shape because of the resonance behaviour of serial resonant tank circuit (L₁₁//L₁, C₁, R_L). When current crosses zero the diode D₁ switches OFF the serial resonant tank circuit. The parallel resonant tank circuit (L₁, C₁) relaxes itself on resistor R_L. When the output voltage v_C crosses zero the diode D₁ becomes switched ON (it has been supposed that triggering pulse on Q₁ is present all the time). The wave-shapes of currents i_{L11} are shown in Fig. 4.

The values of L₁₁ and L₁ have been chosen with intention that the parallel resonant frequency must be 21 kHz, and the serial resonant frequency should assure the soft switching operation in start up procedure.

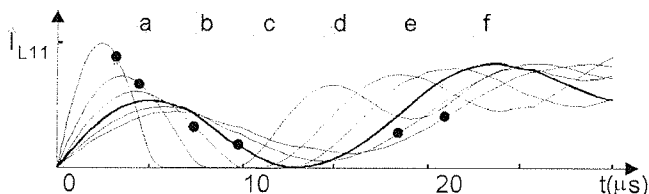


Fig. 4: The soft start analysis.

The wave forms of i_{L11} in Fig. 4 which are marked with "a, b, c, and d" enable the soft switching operation with respect to transistor's current limitation. In steady state there are no problems with soft switching operation because the HF AC link voltage is present. The results in Fig. 4 have been computed by using SPICE simulator.

4. The energy balance consideration

Equations (3) to (7) which describe current i_{L11}, i_{L1} and v_C are very complex. Because of that the design procedure based on energy balance will be described in next lines.

4.1. The Load Requirements

Let us suppose the load is resistance whose power is denoted by P. The peak value of the output voltage is denoted by \hat{V}_m , the frequency of the output voltage is f_p and the peak value of the current through inductance

L₁₁ is denoted by \hat{I}_m . The energy which will supply the load for half of period of the output voltage can be expressed by the next formula:

$$W_{load} = P \frac{T}{2} \quad (8)$$

where T = 1/f_p.

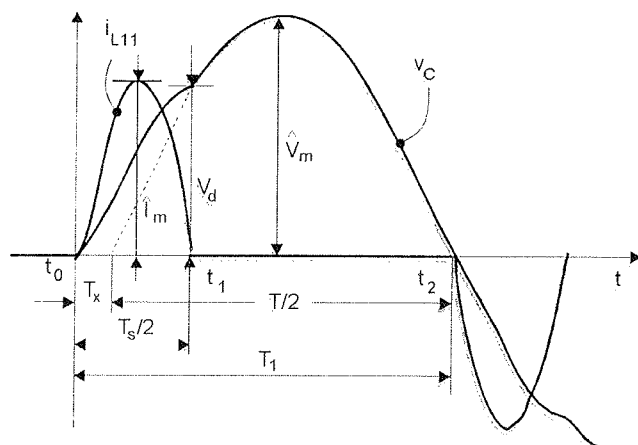


Fig. 5: The waveforms of current and voltage in resonant link converter

That amount of joules has to be stored in parallel resonant tank circuit and in ideal case the energy store in capacitor is:

$$W_C = \int_0^T v_C i_C = W_{load} \quad (9)$$

We can calculate the capacitance C₁, by using (4):

$$C = 2 \frac{W_C}{V_m^2} \quad (10)$$

The inductance L₁ has been calculated by using the expression:

$$L_1 = \frac{1}{4\pi^2 C f_p^2} \quad (11)$$

If the parallel resonant tank circuit has been relaxed (no power supply is connected on circuit), the resistor R_L would be connected on parallel resonant tank circuit. The energy which will be dissipated on the load, can be computed by formula:

$$W_{Diss} = P \left(\frac{T}{2} - \frac{T_s}{2} \right) \quad (12)$$

At the same time that amount of joules is exactly the quantity which has to be provided from DC power supply to parallel resonant tank circuit for each half of period of the output voltage (Fig. 5) in order to get constant output voltage on parallel resonant tank circuit. That yields:

$$W_{LN} = W_{Diss} \quad (13)$$

where W_{LN} describes the energy stored in serial equivalent inductance. This energy W_{LN} has been computed by using the expression:

$$W_{LN} = \int_0^T v_{LN} i_{LN} d\tau \quad (14)$$

For current which will be flown into serial equivalent resonant tank circuits a sinusoidal wave-shape has been supposed (Fig. 5). After time $t = T_s/2$ the energy flow has been stooped.

Expressions for inductor current and voltage yield from next formulas:

$$i_{LN} = \hat{i}_m \sin(\omega_s t) \quad (15)$$

$$v_{LN} = \omega_s \hat{i}_m L_N \cos(\omega_s t) \quad (16)$$

The equations (15) and (16) have been substituted into (14) and yields:

$$W_{LN} = L_N \frac{\hat{i}_m^2}{2} \quad (17)$$

From eq. (17), the equivalent inductance can be defined:

$$L_N = \frac{2W_{LN}}{\hat{i}_m^2} \quad (18)$$

Using (18) we can express the inductance L_{11} :

$$L_{11} = \frac{L_N L_1}{L_1 - L_N} \quad (19)$$

Such computed values for all elements of circuits (Fig. 3) has to be proofed by equations (3) to (7) in order to get soft switch behaviour for current i_{L11} . In the case when the soft switch operation has not been reached, it is necessary to change the ratio between inductance L_{11} and L_1 , which means changing of ratio between energy W_{LN} and W_C .

4.2. The Power Supply Requirements

The above sections show the way of designing the elements of serial and parallel resonant tank circuit from load requirements. In many applications the DC power supply voltage has been forced by mean supply, eq.

(1). On the other hand the peak value of current \hat{i}_m has been proposed for energy balance consideration.

$$\hat{i}_m = f(V_d) \quad (20)$$

This two facts can not be considered together because of connection between that two quantities. The expression (10) has to be found in regard to get a small signal model of such converter as well /5/.

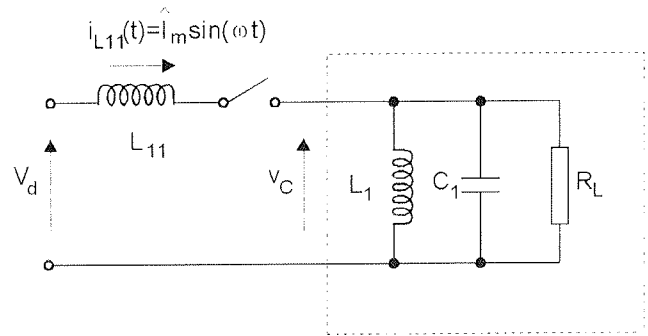


Fig. 6: The equivalent circuit for injected-absorbed current method

Let us suppose that the current i_{L11} and v_C have the wave-shape as shown in Fig. 5. The main current injected from L_{11} into parallel resonant tank circuit (L_1 - C_1 - R_L) is supposed to be sinusoidal.

$$i_{L11} = \hat{i}_m \sin(\omega_{os} t) \quad (21)$$

where ω_{os} is the serial resonant frequency.

On the other hand the derivative of inductance current i_{L11} should be described with the next set of equations:

$$\frac{di_{L11}}{dt} = \frac{1}{L_{11}} [V_d - V_d \sin(\omega_{os} t)] \quad (22)$$

$$\int_0^{\hat{i}_m} di_{L11} = \int_0^{T_s/4} \frac{1}{L_{11}} [V_d - V_d \sin(\omega_{os} t)] dt \quad (23)$$

Which gives us the expression for \hat{i}_m :

$$\hat{i}_m = \frac{T_s}{4L_{11}} V_d \left(1 - \frac{2}{\pi} \right) \quad (24)$$

The equation (14) connects the supply voltage V_d with the magnitude of inductance current \hat{i}_m .

5. The small signal model

According to the classification of analysing methods /5/, the injected-absorbed-current method belongs to the class of the simplest linear methods whose validity is limited to low-frequency, small-signal phenomena. The basic idea that leads to linearization is the introduction of the notation of average values of quantities of interest (usually voltages and currents). Their average values are determined by averaging over a period (duration T) of the switching frequency:

$$q_{av} = \frac{1}{T} \int_{t_1}^{t_1+T} q(t) dt \quad (25)$$

where q represents any quantity of interest and t_1 represents the time at which the averaging process begins. The averaging eliminates the influence of the exact wave forms during the period of the switching frequency, on mathematical relationships among averaged quantities. The result is a dramatic simplification of mathematical expressions in the analysis. Fig. 7 shows the switching cell as a black box.

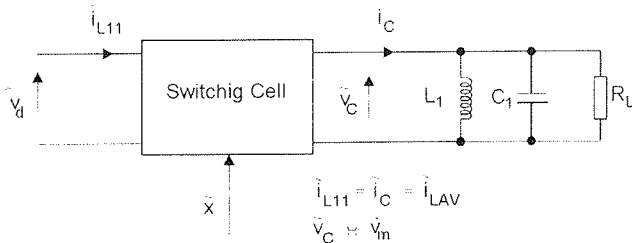


Fig. 7: The switching cell

Five quantities are marked at it's ports: the input voltage and current, the output voltage and current and a fifth quantity x, which is a controlled quantity. Assume now that the average values of the input current i_{L11} can be expressed as functions of the average value x of controlled quantity and the average values of the cell input voltages. The relations:

$$i_{LAV} = i_{LAV}(x, V_d) \quad (26)$$

define these functions.

The average value of current i_{L11} will be denoted by i_{LAV} . From Fig. 5 and 6 follows the next expression:

$$i_{LAV} = \frac{2}{T} \int_0^{T_s/2} \frac{T_s V_d}{4L_{11}} \left(1 - \frac{2}{\pi}\right) \sin(\omega_{os} t) dt \quad (27)$$

$$= \frac{DV_d}{L_{11}(k+1)\omega_{os}} \left(1 - \frac{2}{\pi}\right)$$

In a linear model of the cell, a simple proportional relation among small quantities exists:

$$di_{LAV} = \frac{\partial i_{LAV}}{\partial D} dD + \frac{\partial i_{LAV}}{\partial V_d} dV_d \quad (28)$$

$$= AdD + BdV_d$$

Coefficients A and B are:

$$A = \frac{\partial i_{LAV}}{\partial D} = \frac{V_d}{L_{11}(k+1)\omega_{os}} \left(1 - \frac{2}{\pi}\right)$$

$$B = \frac{\partial i_{LAV}}{\partial V_d} = \frac{D}{L_{11}(k+1)\omega_{os}} \left(1 - \frac{2}{\pi}\right)$$

where $k = 2T_x/T$ (fig. 5).

Unfortunately there is no term to connect the small changing of average value of the input current with the peak value of the output voltage in eq. (28). An inaccurate method is published in /4/. The more accurate method requires that the average value of the output voltage on resonant tank circuit has to be introduced in analyses procedure. From Fig. 5 the half period average value of the output voltage can be evaluated:

$$V_{CAV} = \frac{1}{T_1} \int_0^{T_1} v_C(t) dt =$$

$$\frac{1}{T_1} \left(\int_0^{T_s/2} \hat{V}_d \sin(\omega_{os} t) dt + \int_{T_s/2}^{T_1} \hat{V}_m \sin(\omega_{op} t + \varphi) dt \right) \quad (29)$$

$$= \frac{2V_d D}{\pi(k+1)} + \frac{\hat{V}_m}{2\pi(k+1)} \left[4 - \pi^2(2k^2 + 2kD + D^2) \right]$$

where $\varphi = \omega_{op} T_x$, is a phase angle.

The total differential of the output average voltage was calculated by (30):

$$dV_{CAV} = \frac{\partial V_{CAV}}{\partial V_d} dV_d + \frac{\partial V_{CAV}}{\partial V_m} d\hat{V}_m$$

$$+ \frac{\partial V_{CAV}}{\partial D} dD \quad (30)$$

$$= DdV_d + Ed\hat{V}_m + FdD$$

Where the coefficients D, E, and F are as follows:

$$D = \frac{\partial V_{CAV}}{\partial V_d} = \frac{2V_d}{\pi(k+1)}$$

$$E = \frac{\partial V_{CAV}}{\partial \hat{V}_m} = \frac{1}{2\pi(k+1)} \left(4 - \pi^2(2k^2 + 2kD - D^2) \right)$$

$$F = \frac{\partial V_{CAV}}{\partial D} = \frac{2V_d}{\pi(k+1)} - \frac{\hat{V}_m \pi}{(k+1)} (k+D)$$

Instead of differential quantities dx the small perturbations \tilde{x} has been introduced.

In Fig. 8 the connection between the changing of average current \tilde{i}_{LAV} and it's response - changing of the output voltage \tilde{v}_{CAV} is shown wich means that there is connection between the small perturbations as well.

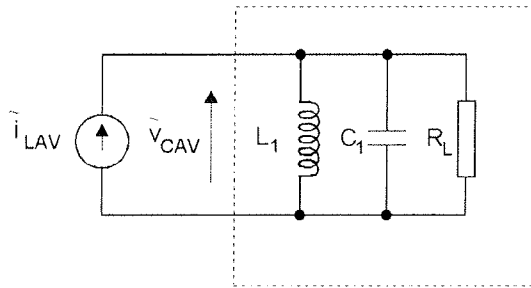


Fig. 8: The Parallel resonant circuit excited by current generator instead of voltage source, serial inductance and semiconductor switch

The voltage on the parallel resonance tank circuit is:

$$\tilde{v}_{CAV}(s) = \frac{sL_{11}}{s^2L_{11}C + s\left(\frac{L_{11}}{R}\right) + 1} \tilde{i}_{LAV}(s) \quad (31)$$

$$= Z(s)\tilde{i}_{LAV}(s)$$

After taking the Laplace transform of eq. (28) and (30) and eq. (28) into (31), regarding to eliminate \tilde{i}_{LAV} and \tilde{v}_{CAV} , we get the following equation:

$$\tilde{v}_m = \frac{1}{E} [(A\tilde{d} + B\tilde{v}_d)Z(s) - D\tilde{v}_d - F\tilde{d}] \quad (32)$$

The transfer function $\frac{\tilde{v}_m(s)}{\tilde{d}(s)}$ was calculated by using eq.

(32) with presumption that $\tilde{v}_d = 0$, which yields:

$$\frac{\tilde{v}_m(s)}{\tilde{d}(s)} = -\frac{1}{E} \frac{FL_1Cs^2 + s\left(\frac{L_1}{R} - AL_1\right) + 1}{s^2L_1C + s\left(\frac{L_1}{R}\right) + 1} \quad (33)$$

From eq. (33) the magnitude and phase of the transfer function can be computed. Fig. 10 (a), (b) show the magnitude and phase frequency responses.

The control object (Fig. 9) consist of PWM block as well. A frequency response of PWM was published in /4/.

From eq. (34) the magnitude and phase of the PWM transfer function can be computed. The frequency response of PWM and of whole object are shown in Fig. 10 (c),(d) and (e),(f) respectively. A design of control parameter has been done in frequency domain.

$$\frac{\tilde{d}(s)}{\tilde{u}_{kr}(s)} = \frac{K}{\tilde{V}_m} \frac{1}{sT_s + 1} \quad (34)$$

where $K = \frac{1}{2\pi} \cos^{-1}\left(-\frac{V_d}{\tilde{V}_m}\right) \frac{T}{T_x} - 1.$

5. The experimental results

The experimental results confirm our theoretical model of the AC to HF-AC Resonant Link Converter where a control of the peak value of the high frequency output voltage was achieved. The proposed control scheme is described in Fig. 9.

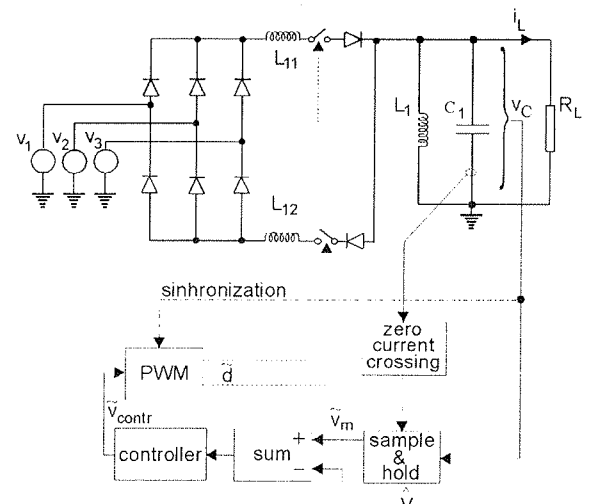


Fig. 9: The control sheme

The S&H circuit is used instead of the peak detector. The capacitor current i_c has a delay versus voltage v_c exactly 90° el. If the voltage is sampled in that time instant (when the current i_c crosses zero), the peak value of voltage v_c will be measured. That simple phenomena helped, that there are any filter in measuring circuit. The delay will be one period of the output voltage.

6. Conclusion

The main idea which has been discussed in this article is providing the energy through serial resonant tank circuit into parallel resonant tank circuit. By substitution the diode rectifier and main supply instead of DC voltage the "new" circuit was introduced. In order to use snubberless circuit the start up problem has to be solved by manipulations with values of L_{11} and L_1 . The main effort has been done at the efficiency analysis and consequently the efficiency increases up to 92%. There are no switching losses, but there are core and copper losses in inductance and conducting losses in transistors and diodes. With introduction of the Injected-Absorbed-Current method of analysis the linearized transfer function has been developed for AC to /HF-AC resonant link converter.

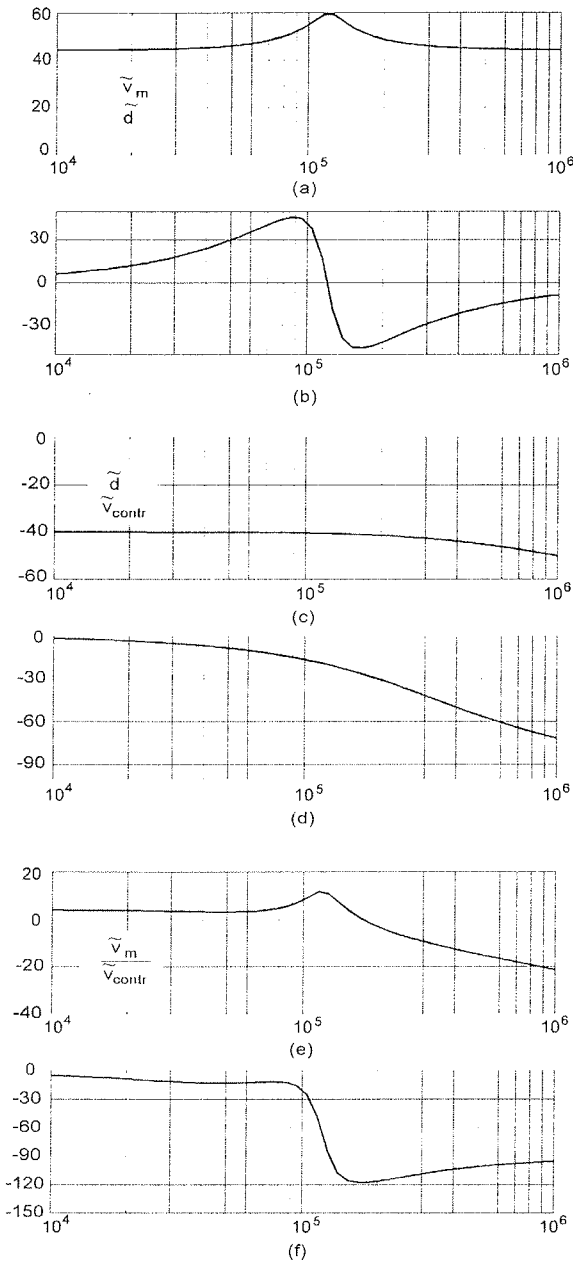


Fig. 10: The frequency responses

References

- /1/ P.K. Sood, T.A. Lipo, "Power Conversion Distribution System Using a Resonant High Frequency AC Link", IEEE IAS Trans., vol. 24, pp. 586-596, March/April 1988.
- /2/ D.M. Divan, "The Resonant Link Inverter, a New Concept in Power Conversion", IEEE-IAS Annual Meeting Conf. Rec. 1986 pp. 648-656.
- /3/ S.K. Sul, T.A. Lipo, "Design and Performance of a High Frequency Link Induction Motor Drive Operating at Unity Power Factor", IEEE IAS Annual Meeting, Proc., pp. 308-313, Oct. 1988.
- /4/ M. Milanović, D. Zdravec, A. Hren, F. Mihalič, "DC to HF-AC Resonant Link Converter by Using Serial and Parallel Resonance", IEEE PEDS Conference, Singapore Feb. 1995.
- /5/ A.S. Kislowski, R. Redl, N.O. Sokal, Dynamic Analysis of Switching-Mode DC/DC Converters, Van Nostrand Reinhold, New York 1991.

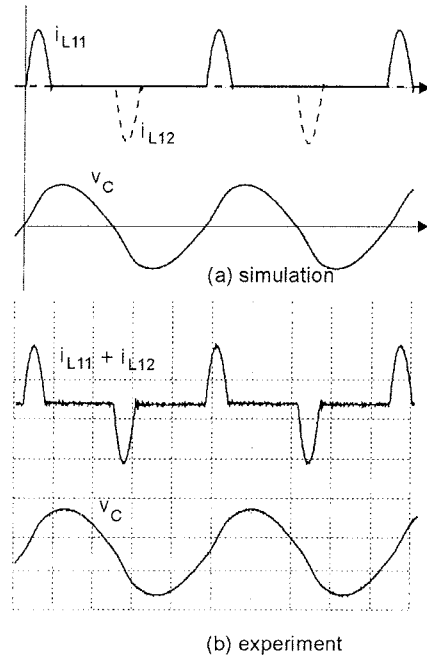


Fig. 11: (a) simulation results; currents i_{L11} , i_{L12} and voltage v_C , (b) experimental results i_{L1}, i_{L11} (1 A/div) and voltage v_C (50 V/div), time axis 10 μ s/div

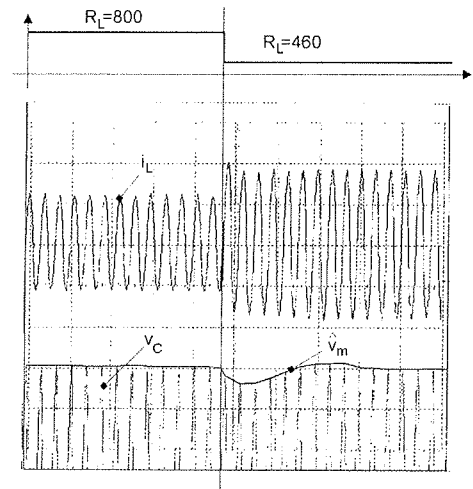


Fig 12: The experimental results: i_L , x-axis 100 μ s/div, y-axis 0.2 A/div, v_C , $V_{p-p}=300$ V, x-axis 100 μ s/div, y-axis 20V/div.

izr.prof. dr. Miro Milanović
Robert Kovačić, dipl.ing.
mag. Franc Mihalič, dipl.ing.
doc.dr. Rudi Babič
University of Maribor
Faculty of Electrical Engineering
and Computer Science
Smetanova 17
2000 Maribor
tel.: +386 62 221-112
fax: +386 62 273-578

Prispelo (Arrived): 01.02.1996

Sprejeto (Accepted): 27.02.1996